

PCCP

Accepted Manuscript



This is an *Accepted Manuscript*, which has been through the Royal Society of Chemistry peer review process and has been accepted for publication.

Accepted Manuscripts are published online shortly after acceptance, before technical editing, formatting and proof reading. Using this free service, authors can make their results available to the community, in citable form, before we publish the edited article. We will replace this *Accepted Manuscript* with the edited and formatted *Advance Article* as soon as it is available.

You can find more information about *Accepted Manuscripts* in the [Information for Authors](#).

Please note that technical editing may introduce minor changes to the text and/or graphics, which may alter content. The journal's standard [Terms & Conditions](#) and the [Ethical guidelines](#) still apply. In no event shall the Royal Society of Chemistry be held responsible for any errors or omissions in this *Accepted Manuscript* or any consequences arising from the use of any information it contains.

Viscosity Scaling of the Self-diffusion and Velocity Cross-correlation Coefficients of Two Functionalised Ionic Liquids and of their Non-functionalized Analogues.[†]

Kenneth R. Harris,

School of Physical, Environmental and Mathematical Sciences,

University College, University of New South Wales,

PO Box 7916, Canberra BC, ACT 2610, Australia,

and

Takashi Makino and Mitsuhiro Kanakubo

National Institute of Advanced Industrial Science and Technology (AIST),

4-2-1 Nigatake, Miyagino-ku, Sendai 983-8551, Japan.

[†] Supplementary information (ESI) available: numerical tables of experimental diffusion coefficients as a function of temperature, derived velocity correlation and distinct diffusion coefficients, and Nernst-Einstein deviation parameters.

Abstract :

Ion self-diffusion coefficients have been measured for ionic liquids based on the cations *N*-acetoxyethyl-*N,N*-dimethyl-*N*-ethylammonium ($[N_{112,20CO1}]^+$) and its non-functionalised analogue, *N,N*-dimethyl-*N*-ethyl-*N*-pentylammonium ($[N_{1125}]^+$), and *N,N*-dimethyl-*N*-ethyl-*N*-methoxyethoxyethylammonium ($[N_{112,202O1}]^+$), and its analogue, *N,N*-dimethyl-*N*-ethyl-*N*-heptylammonium ($[N_{1127}]^+$) and the bis(trifluoromethanesulfonyl)amide anion. The functionalised chain on an ammonium cation has the same length, in terms of the number of atoms, as the non-functionalised chain of the corresponding analogue. For $[N_{112,20CO1}][Tf_2N]$ and $[N_{1127}][Tf_2N]$, the cation and anion self-diffusion coefficients are equal, within experimental error, whereas for $[N_{1125}][Tf_2N]$, the cation diffuses more quickly, and for $[N_{112,202O1}][Tf_2N]$, it is the anion that diffuses more quickly than the ether-functionalised cation. But these differences are relatively small, just beyond experimental error. The data are used to calculate velocity cross-correlation coefficients (VCC or f_{ij}) and distinct diffusion coefficients (D_{ij}^d). Both the self-diffusion and distinct diffusion coefficients are analysed in terms of (fractional) Stokes-Einstein-Sutherland equations. Though the self-diffusion coefficients, as with the conductivity and viscosity, show marked differences in absolute terms between the functionalised and non-functionalised forms, being higher for the ethoxy-substituted IL and lower for the acetoxy-substituted IL, these are largely removed by scaling with the viscosity. Thus the transport properties are better understood as functions of the viscosity rather than the temperature and density, *per se*. The presence of the alkoxy-substituted side chains is known to change the local mesoscopic liquid structure, but it appears once this is done, the transport properties scale correspondingly. In the case of the acetoxy-substituted IL, this is also largely the case, but the the Nernst-Einstein deviation parameter, Δ , which depends

on the difference between the anion-cation VCC and the mean of the cation-cation and anion-anion VCCs, is smaller than that of its analogue salt, and also temperature dependent.

Introduction

One of the questions asked about ionic liquids is “*how do the transport properties depend on the nature and structure of the constituent ions?*” In any industrial application, costs of plant design and operation are in part dependent on the viscosity and the thermal conductivity of the liquid systems employed, along with thermodynamic properties such as the heat capacity, as these govern energy and mass transfer.¹ In addition, electrochemical applications may also require knowledge of the electrical conductivity, transport numbers and oxidation and reduction potentials. Though there are now numerous measurements of ionic liquid viscosity, somewhat fewer of ion intra- or self-diffusion, fewer still of electrical conductivity and an even smaller number of studies of thermal conductivity, our knowledge of these inter-related properties needs to be integrated and the relationship with structure and, in particular, the effect of functionalisation determined, in order to answer the question above and hence allow optimization of ionic liquid applications.

Some initial studies have been made, both computational and experimental. Tang et al.² have reviewed the literature for ether and alcohol functionalised ionic liquids and Rollet and Bessada³ have reviewed self-diffusion measurements, both to 2011. It is now known that lengthening alkyl substituents on cations tends to increase the viscosity and decrease the conductivity,^{4,5,6} as does reducing the symmetry of the anion.² The insertion of alkoxy and alkoxyalkyl groups on cations tends to reduce the viscosity,^{2,7,8,9,10} an effect long known for molecular liquids.^{11,12} Similarly, such substitution generally lowers the electrical conductivity of ionic liquids. However, counter examples have been reported,² with, for example, 1-methoxy-3-methylimidazolium tetrafluoroborate having a higher viscosity than its non-functionalised analogue,¹³ and methoxymethyl-ethyl-dimethylammonium

tetrafluoroborate as having a particularly low conductivity.¹⁴ On the other hand, the introduction of hydroxyl groups on alkyl substituents usually increases the viscosity.²

Other studies include that of Niedermeyer et al.¹⁵ who used *ab initio* theoretical studies of ion pairs, combined with IR spectroscopy and X-ray crystallography, to investigate the effect of a siloxy group substituted on an imidazolium ring cation on the viscosity. It was found that the flexibility of the siloxane linkage lowered barriers to internal rotation within the substituent chain allowing easier inter-conversion of cation conformers and hence freer movement of the anion around the cation. This was used to infer a lower viscosity for 1-methyl-3-pentamethyldisiloxymethylimidazolium chloride, [(SiOSi)C₁C₁im]Cl, than for 1-methyl-3-butylimidazolium chloride, [C₄C₁im]Cl, despite the near-equivalence of the ion-pairing energies in the two salts.

In a computational study of the effect of the replacement of an alkyl by an alkoxy chain in a quaternary ammonium ionic liquid similar to the salts studied here, Siqueira and Ribeiro¹⁶ found that the *N*-ethyl-*N,N*-dimethyl-*N*-(2-methoxyethyl)ammonium bis(trifluoromethanesulfonyl)amide, [N_{112,201}][Tf₂N] (in our notation), had lower viscosity, and higher ion self-diffusion coefficients and conductivity, than its non-functionalised analogue, the *N*-ethyl-*N,N*-dimethyl-*N*-butyl salt, [N₁₁₂₄][Tf₂N]. The difference was attributed to stronger short-ranged association between neighbouring cations in the latter salt.

In another computational work, functionalisation of the anion was examined. Kowsari et al.¹⁷ used molecular dynamics simulations to calculate ion diffusion coefficients and electrical conductivities for amino acid salts of the tetrabutylphosphonium ion. As well as determining the effects of ion velocity cross-correlations,¹⁸ Kowsari et al. found that the introduction of acid or amide polar

functional groups on the amino acid anion side chain decreased the ion self-diffusion coefficients as well as the conductivity.

There are also some experimental studies not included in Tang's survey. Matsumoto and co-workers¹⁹ determined the effect of varying the lengths and symmetry of bis(perfluoroalkanesulfonyl)amide ions of ionic liquids with substituted ammonium and 1-ethyl-3-methyl imidazolium cations, though the study was restricted to a single temperature. They found that the logarithm of viscosity varied approximately with the molar volume of the ionic liquid for a given cation, and that the corresponding points on a Walden plot of molar conductivity against viscosity followed the same order. A similar result has been obtained by Yoshida and Saito²⁰ for diethylmethyl-(2-methoxyethyl)ammonium ($[\text{N}_{122,201}]^+$) bis(perfluoroalkanesulfonyl)amides. A second study from the Matsumoto group²¹ found that an ether linkage in an anion shows the same viscosity reduction and conductivity enhancement as in cations, and, in addition, the self-diffusion coefficients of both anion and cation are increased relative to the non-functionalised analogue.

Shirota et al.⁷ have also compared certain phosphonium-based ionic liquids with the ammonium analogues, and hexafluoroarsenates with the corresponding hexafluorophosphates. Phosphonium-based ionic liquids generally have higher conductivity and a lower viscosity than their ammonium-based analogues.^{22,23,24}

In a previous paper by two of the present authors and coworkers, the temperature dependences of the viscosity and electrical conductivity of four ionic liquids with substituted ammonium cations and the bis(trifluoromethanesulfonyl)amide anion ($[\text{Tf}_2\text{N}]^-$) were reported.²⁵ The cations were *N*-acetoxyethyl-*N,N*-dimethyl-*N*-ethylammonium ($[\text{N}_{112,20\text{CO}_1}]^+$) and its non-

functionalised analogue, *N,N*-dimethyl-*N*-ethyl-*N*-pentylammonium ($[N_{1125}]^+$), and *N,N*-dimethyl-*N*-ethyl-*N*-methoxyethoxyethylammonium ($[N_{112,20201}]^+$), and its analogue, *N,N*-dimethyl-*N*-ethyl-*N*-heptylammonium ($[N_{1127}]^+$) (Figure 1). The functionalised chain on the ammonium cations has the same length, in terms of the number of atoms, as the non-functionalised chain of the corresponding analogue. The ester functionalised ionic liquid $[N_{112,20CO1}][Tf_2N]$, was found to have poorer transport properties, that is a higher viscosity and a lower electrical conductivity and molar conductivity than those of $[N_{1125}][Tf_2N]$, at a given temperature. Consistent with the discussion above, and work on pyrrolidinium-based ionic liquids,²⁶ the ether functionalised ionic liquid $[N_{112,20201}][Tf_2N]$, had superior transport properties to $[N_{1127}][Tf_2N]$.

As is well known, scaling conductivities as a function of viscosity reduces apparent differences observed at given state points (T, p). At 80 °C, the spread in molar conductivities for the ionic liquids listed above is 229 ($[N_{1127}][Tf_2N]$) to 432 S $m^2 mol^{-1}$ ($[N_{112,20201}][Tf_2N]$). At 10.4 mPa s, the viscosity of $[N_{1127}][Tf_2N]$ at 80 °C, the spread in molar conductivities is somewhat less, approximately 100 S $m^2 mol^{-1}$, $[N_{1127}][Tf_2N]$ having the smallest value and the ester functionalised $[N_{112,20CO1}][Tf_2N]$ the highest, an intriguing result. This is represented in the Walden plots, Figure 2: note that the log-log plots are linear (a test of the quality of the data), but that this is at the expense of being able to resolve small differences. The lines for $[N_{112,20201}][Tf_2N]$ and $[N_{1125}][Tf_2N]$ are almost superposable on one another. The slopes are very nearly equal, almost within experimental error, the standard deviation being ± 0.002 .

We have made several studies of the transport properties of ionic liquids, including the viscosity, ion self-diffusion coefficients and the electrical conductivity. A major result has been that the self-diffusion coefficients (D_i) and the molar

conductivity (Λ) depend on the viscosity (η) in a regular way, such that the slopes of Stokes-Einstein-Sutherland plots for the self-diffusion coefficients and that of a Walden plot have, for a given ionic liquid, similar fractional, slopes.^{27,28} Both self-diffusion coefficients and the molar conductivity are functionals of Kubo velocity correlation functions²⁹ and therefore can be used to calculate both velocity cross-correlation coefficients and distinct diffusion coefficients, D_{ij}^d ($i,j = +,-$),³⁰ for like ion (cation-cation and anion-anion) and unlike ion (cation-anion) interactions.^{27,28,31,32,33} These latter also show similar fractional slopes when plotted in the Stokes-Einstein-Sutherland/Walden form.^{18,27,28,31} In both these plots, whether of the experimentally measured transport coefficients or of the derived distinct diffusion coefficients, data points for a given ionic liquid on high pressure isotherms fall on the same line as points on the atmospheric pressure isobar. The conclusion is that those transport properties that are functionals of Kubo velocity correlation functions (D_i and Λ) scale with the viscosity, not temperature or pressure *per se*. Thus an ion self-diffusion coefficient or the conductivity is set by the viscosity and the Stokes-Einstein-Sutherland and Walden equations thus provide useful, though still empirical, scaling functions. This scaling can then be utilised to compare the behaviour of functionalised ionic liquids with their non-functionalised counterparts.

A first step in this direction has been taken in a collaboration with CSIRO Energy Technology colleagues where the molar conductivity, ion self-diffusion and distinct diffusion coefficients of two closely related *N*-donor functionalised quaternary ammonium ionic liquids with bis(trifluoromethanesulfonyl)amide anions, the cyclic 1-ethyl-1,4-dimethyl-piperazinium bis(trifluoromethanesulfonyl)amide and its open chain analogue 1-(2-dimethylaminoethyl)dimethylethylammonium bis(trifluoromethanesulfonyl)amide were also found to scale very similarly, though

not identically, with the viscosity despite the different cation structures.³³ The scaling was not greatly different to that for the non-functionalised *N*-butyl-*N*-methylpyrrolidinium bis(trifluoromethanesulfonyl)amide,³¹ an unexpected result. It suggests that while the absolute transport property values may be affected by functionalisation, these scale similarly with the viscosity, at least for these examples.

There are similar trends in Walden plots for ionic liquids with substituted pyridinium and pyrrolidinium cations (structures, Figure 3). Figure 4 shows plots calculated for the pair *N*-butylpyridinium bis(trifluoromethanesulfonyl)amide ([Py₄][Tf₂N]) (density, viscosity³⁴; conductivity³⁵) and *N*-(2-hydroxyethyl)pyridinium bis(trifluoromethanesulfonyl)amide ([Py_{2OH}][Tf₂N])³⁶ and the trio *N*-butyl-*N*-methylpyrrolidinium bis(trifluoromethanesulfonyl)amide ([Pyr₁₄][Tf₂N])²⁶ and *N*-(2-methoxymethyl) *N*-methylpyrrolidinium bis(trifluoromethanesulfonyl)amide ([Pyr_{1,101}][Tf₂N])²⁶ and *N*-(2-methoxyethyl) *N*-methylpyrrolidinium bis(trifluoromethanesulfonyl)amide ([Pyr_{1,102}][Tf₂N]) (density, viscosity³⁷; conductivity³⁸). The (Walden) lines for the first pair (slopes $t = 0.927, 0.941$ respectively) lie close together (and are almost coincident with that for [Pyr₁₄][Tf₂N]), but those for the trio are spaced further apart, (slopes $t = 0.924, 0.928$ and 0.931 respectively) with the ether-substituted IL having a lower conductivity at a given viscosity than its analogue. Also plotted in the third panel are data for the bis(fluorosulfonyl)amide (FSA) salts of the [Pyr₁₄]⁺ and [Pyr_{1,101}]⁺.²⁶ The smaller [FSA]⁻ anion gives a higher conductivity at a given viscosity compared to the larger [Tf₂N]⁻. This is consistent with results from studies of both conductivity and ion self-diffusion coefficients for 1-ethyl-3-methylimidazolium ([emim]⁺)³⁹ and *N*-methyl-*N*-propylpyrrolidinium ([Pyr₁₃]⁺)⁴⁰ salts by Hayamizu and her co-workers, though it

should be noted that somewhat lower t values are found for the latter salts {0.78 ([Py_{r13}][FSA]) and 0.80 ([Py_{r13}][Tf₂N])} than for those discussed here.

Here we extend this viscosity scaling approach to examine the four ammonium cation bis(trifluoromethanesulfonyl)amide ionic liquids studied by Makino et al.²⁵ using ion self-diffusion coefficients measured by the steady gradient spin-echo NMR method and velocity correlation and distinct diffusion coefficients calculated from these and the molar conductivities.

Experimental

The steady-gradient spin-echo NMR self-diffusion apparatus and its calibration and application to ionic liquids have been described in previous work.^{27,28,31,33} This technique avoids the artefacts sometimes found with pulsed field gradient methods when applied to viscous ionic liquids.^{40,41,42} As is usual for ionic liquids, the temperature range that could be covered by our apparatus was limited by the short T_2 relaxation times, which also attenuate the signal in addition to diffusion, with greater effect at lower temperatures. The fixed, upper limit of the apparatus was 90 °C. The estimated uncertainty in D is $\pm 4\%$ (due to the low signal to noise ratios obtaining in these systems) and ± 0.05 K in the temperature.

The preparation of the sample materials was described in the work on the density, viscosity and conductivity.²⁵ The samples, prepared in Sendai, were sealed in evacuated 5 mm NMR tubes for the diffusion measurements in Canberra. Such dry and out-gassed samples, in the case of the imidazolium salts, have been found to be stable for five years and more. The molar masses and water content are given in Table 1.

The measured self-diffusion coefficients (D) are given in Table S1 (Supplementary Information) and the derived velocity cross-correlation coefficients, f_{ij} , distinct diffusion coefficients, D_{ij}^d , and values of the Nernst-Einstein deviation parameter, Δ , in Table S2. The diffusion coefficients were fitted to the standard Vogel-Fulcher-Tammann equation,

$$D = \exp[A + B / (T - T_0)] \quad (1)$$

and the Litovitz equation,

$$D = \exp(A' + B' / T^3) \quad (2)$$

Fitting parameters are given in Tables 2 and 3. Makino et al.²⁵ noted that the Litovitz equation gave poor fits for the viscosity and molar conductivity for the four ionic liquids considered here (their Figures 2 and 4): this is less noticeable for the diffusion coefficients as the precision is less and the temperature ranges shorter than for the viscosity and molar conductivity results. The worst case is D_+ for $[\text{N}_{1125}][\text{Tf}_2\text{N}]$.

Discussion

At a given temperature, the diffusion coefficients have magnitudes in the order $[\text{N}_{112,20201}][\text{Tf}_2\text{N}] > [\text{N}_{1125}][\text{Tf}_2\text{N}] > [\text{N}_{1127}][\text{Tf}_2\text{N}] \sim [\text{N}_{112,20\text{CO}1}][\text{Tf}_2\text{N}]$ (Table S1 and Figure 5). This is similar to the order for the molar conductivity, $[\text{N}_{112,20201}][\text{Tf}_2\text{N}] > [\text{N}_{1125}][\text{Tf}_2\text{N}] > [\text{N}_{112,20\text{CO}1}][\text{Tf}_2\text{N}] > [\text{N}_{1127}][\text{Tf}_2\text{N}]$, but not that for the fluidity ($\phi = 1/\eta$), where $[\text{N}_{112,20201}][\text{Tf}_2\text{N}] > [\text{N}_{1125}][\text{Tf}_2\text{N}] > [\text{N}_{1127}][\text{Tf}_2\text{N}] > [\text{N}_{112,20\text{CO}1}][\text{Tf}_2\text{N}]$.²⁴ Thus, the salt with the ether-functionalised cation has the highest diffusion coefficients, molar conductivity and fluidity, a similar result to that found in the molecular dynamics study of $[\text{N}_{112,201}][\text{Tf}_2\text{N}]$ and $[\text{N}_{1124}][\text{Tf}_2\text{N}]$ ¹⁶ and the experimental study of Umecky et al.,¹⁹ (both constrained to single temperatures),

whereas that with the ester-functionalised cation has the lowest diffusion coefficients and fluidity, but not molar conductivity, which is that of $[\text{N}_{1127}][\text{Tf}_2\text{N}]$.

For $[\text{N}_{112,20\text{CO}1}][\text{Tf}_2\text{N}]$ and $[\text{N}_{1127}][\text{Tf}_2\text{N}]$, the cation and anion self-diffusion coefficients are equal, within experimental error, whereas for $[\text{N}_{1125}][\text{Tf}_2\text{N}]$, the cation diffuses more quickly, and for $[\text{N}_{112,20201}][\text{Tf}_2\text{N}]$, it is the anion that diffuses more quickly than the ether-functionalised cation. But these differences are relatively small, just beyond experimental error.

There appear to be no previous measurements for self-diffusion in these ionic liquids, though there are for the closely related *N,N*-diethyl-*N*-methyl-*N*-(2-methoxyethyl)ammonium bis(trifluoromethanesulfonyl)amide, $[\text{N}_{122,201}][\text{Tf}_2\text{N}]$.⁴³ These are slightly higher than our results for $[\text{N}_{112,20201}][\text{Tf}_2\text{N}]$ (Figure 5).

Some workers have attempted to find correlations for ionic liquid transport properties as a function of volume.^{44,45} Though the group of ionic liquids studied here are structurally similar, and have a common anion, they have very different molar volumes, varying from 316 to 350 cm³/mol (Table 1). It is known that transport properties of liquids can be scaled with temperature and density as $[TV^\gamma]$, where γ is related to the repulsive part of the intermolecular potential, being $n/3$ for model fluids interacting with a simple inverse power law potential with exponent n .⁴⁶ Though such scaling is regarded by theoreticians as only approximate,⁴⁷ and strictly speaking inapplicable to molten salts that interact through Coulombic forces in addition to Van der Waals forces, such scaling empirically is found to work quite well, with γ values for ionic liquids of the order of 1 to 4.⁴⁸ However, such an analysis requires high pressure data obtained over broad ranges of temperature and density; consequently it cannot be applied here.

Instead it seems more fruitful to examine scaling of the diffusion coefficients and the conductivity with the viscosity. As with the majority of ionic liquids, Walden plots for these substances are fractional, that is,

$$\Lambda \eta^t = \text{const} \quad (3)$$

with $t < 1$ (Figure 2). Consequently, direct plots of molar conductivity as a function of viscosity are non-linear (see also Martinelli et al.⁶). As mentioned in the Introduction, we have used velocity cross-correlation coefficients (VCC or f_{ij} , $i, j = +, -$) as an aid to interpreting ionic liquid transport coefficients.^{27,28,31-33} These are related to the experimental transport properties through the equations

$$f_{++} \equiv \frac{N_A V}{3} \int_0^\infty \langle v_{+\alpha}(0) v_{+\beta}(t) \rangle dt = RT \kappa \left(\frac{M_-}{z_- F c M} \right)^2 - \frac{D_+}{v_+ c} \quad (4)$$

(with an analogous form for anion-anion velocity correlations) and

$$f_{+-} \equiv \frac{N_A V}{3} \int_0^\infty \langle v_{+\alpha}(0) v_{-\beta}(t) \rangle dt = RT \kappa \frac{M_+ M_-}{z_+ z_- (F c M)^2} \quad (5)$$

where N_A is the Avogadro constant, F the Faraday, V the volume of the ensemble, κ is the conductivity, c the amount concentration (molarity) of salt, t time, v_i are ion velocities, z_i and ν_i are (signed) charge and stoichiometric numbers, and M , M_+ , and M_- are the molar masses of salt, cation, and anion, respectively. As emphasised by Kashyap et al.,⁴⁹ the VCC are negative quantities for 1-component molten salts, so the ensemble averaged ion velocities are *anti*-correlated due to the principle of momentum conservation. This contrasts with the situation of ions in electrolyte solutions where momentum is also distributed among the solvent molecules and, in consequence, the VCC may be positive or negative.⁵⁰ It has been found that for a number of imidazolium salts^{27,28} and a pyrrolidinium salt³¹ that the VCC are functions of the viscosity over a range of temperature and pressure, that is, high-pressure

isotherms and atmospheric pressure isobars fall on common curves. In other words, the VCC scale with the viscosity. (This is not the case for aqueous electrolytes.)

When the VCC are converted to distinct diffusion coefficients, D_{ij}^d ,^{30,31-33} (these are also negative quantities), through the identity

$$D_{ij}^d = \epsilon f_{ij} (v_+ + v_-) \quad (6)$$

one can express the viscosity-scaling of the VCC in terms of analogues of Stokes-Einstein-Sutherland and Walden plots. Indeed it can be seen from eq. (5) and (6) that a plot of $\ln(-D_{+/-}^d/T)$ against $\ln(1/\eta)$ is in fact a Walden plot, given $A = \kappa/c$. Figures 6 and 7 are Stokes-Einstein-Sutherland plots of the ion self-diffusion coefficients and the distinct diffusion coefficients respectively. The figures show a fractional Stokes-Einstein-Sutherland dependence.

There is a close correlation of the diffusion coefficients with the viscosity for the cations and anions of the two closely related pairs of salts, [N₁₁₂₅][Tf₂N] and [N_{112,20CO1}][Tf₂N], with five-core-atom side-chains, Figure 6a, and, [N₁₁₂₇][Tf₂N] and [N_{112,202O1}][Tf₂N], with seven-core-atom side-chains, Figure 6b. In essence, by scaling with the viscosity, the differences between members of each pair apparent in Figure 5 are largely removed. All four plots have the same slope, t , within experimental error, an average of 0.98 (see Table 4), slightly higher than that for the Walden plot, 0.94. The diffusion data of Hayamizu et al.⁴³ for [N_{122,201}][Tf₂N] are included, utilizing the viscosity data of Yoshida and Saito²⁰ (only available for the limited temperature range 20 - 70 °C): these overlie our results, so the slight difference in the structure of the ether substituted ionic liquids (one methyl- and two ethyl- moieties versus two methyl- and one ethyl-) makes no difference to the plot.

The velocity cross-correlation coefficients themselves follow the order $f_{-} < f_{++} < f_{+-}$ for each salt (see Table S2), consistent with our results for other [Tf₂N]⁺ based

ionic liquids.^{28,31,32} The spread in t for the like-ion velocity correlations is greater than for the self-diffusion coefficients alone due to the combination of self-diffusion coefficients with conductivities to produce the VCC, whereas the values for f_{+-} are unchanged from that of the Walden plot. Moreover when the distinct diffusion coefficients for the ether-functionalised salt $[\text{N}_{112,20201}][\text{Tf}_2\text{N}]$ are scaled with the viscosity, they closely overlap those for the non-functionalised analogue, $[\text{N}_{1127}][\text{Tf}_2\text{N}]$ (see Figure 7b and Table 5). However, in the comparison of the ester functionalised salt $[\text{N}_{112,20\text{CO}1}][\text{Tf}_2\text{N}]$ with its non-functionalised analogue, $[\text{N}_{1125}][\text{Tf}_2\text{N}]$, the scaling does not produce exact overlap for the cation-cation and cation-anion velocity correlations (Figure 7a), with the ester-functionalised salt having a slightly lower cation-cation f_{++} and D_{++}^d than its non-functionalised analogue and the opposite order for the cation-anion f_{+-} and D_{+-}^d . [n.b. $\ln(-D_{ij}^d/T)$ is plotted, so the order $f_{-} < f_{++} < f_{+}$ is reversed on the graphs]. Consequently, in terms of velocity cross-correlations at fixed viscosity, adding an ether moiety to the alkyl chain of a ammonium salt has almost no effect, while adding an ester functionality induces a small change. Again, the differences shown in Figure 5, where the properties are unscaled, are nevertheless greatly reduced for both pairs.

These results reinforce the conclusion of our recent work on N-donor functionalised ionic liquids,³³ where open chain ions were compared with both functionalised and non-functionalised cyclic counterparts, that while the the transport properties of ionic liquids with similar structures may differ considerably in their absolute values at a given temperature (and pressure), by and large, they tend to scale similarly with the viscosity. Whether this behaviour is more general than for the examples we have been able to examine remains to be seen, but our results do suggest that in designing a series of ionic liquids with similar structures for, say, a given

viscosity, one can expect the conductivity to correspond in proportion, lying close to the limits given by distinct diffusion coefficient – viscosity plots for any particular given member of the series. It is particularly interesting that this seems thus far the case only when the structures of cations are varied: variation of the anion seems to have a more marked effect, as comparison of the distinct diffusion coefficients of 1-methyl-3-butylimidazolium BF_4^- , PF_6^- and Tf_2N^- salts shows (see Figure 2 of ref. 31) where $f_{++} < f_- < f_+$ for the two former salts, but $f_- < f_{++} < f_+$ for the latter.

The Nernst-Einstein equation links conductivities with ion self-diffusion coefficients.

$$\Lambda = (F^2 / RT)(v_+ z_+^2 D_+ + v_- z_-^2 D_-)(1 - \Delta) \quad (7)$$

Deviations from the simple NE expression ($\Delta = 0$) occur due to differences in cross-correlation functions of ionic velocities and it has been shown elsewhere that the NE deviation parameter can be expressed directly in terms of the velocity cross-correlation coefficients (VCC or f_{ij}) for like-ion and unlike-ion interactions.^{18,27, 28}

Thus

$$\begin{aligned} \Delta &= - \frac{c (2v_+ v_- z_+ z_- f_{+-} + 2v_+^2 z_+^2 f_{++} + 2v_-^2 z_-^2 f_{--})}{(v_+ z_+^2 D_+ + v_- z_-^2 D_-)} \\ &= \frac{2c [f_{+-} - (f_{++} + f_{--}) / 2]}{(D_+ / v_+ + D_- / v_-)} \end{aligned} \quad (8)$$

In the literature it is often assumed that non-zero values of Δ imply some sort of ion-pairing, but this is incorrect^{18, 31, 32, 49} and may be due to a misinterpretation of a quasi-lattice model of activated jumps due to Bockris et al.^{51, 52} that has persisted despite Bockris' criticism of the assumption of ion-pairing.⁵² Eq. 8 clearly shows that Δ is only zero if there is a fortuitous cancelling of f_{+-} with the mean of f_{++} and f_{--} . More importantly, Δ depends on the difference between these quantities, and experiment and molecular dynamics simulations show it is always less than unity, and typically

lies between 0.2 and 0.4 for ionic liquids, as is the case here for $[\text{N}_{1125}][\text{Tf}_2\text{N}]$, $\Delta \sim 0.42$, $[\text{N}_{112,20201}][\text{Tf}_2\text{N}]$, $\Delta \sim 0.38$ and $[\text{N}_{1127}][\text{Tf}_2\text{N}]$, $\Delta \sim 0.37$ (Figure 9 and Table S2). For these three liquids, Δ is independent of temperature within experimental error (± 0.05), though it looks likely that the latter has some temperature dependence, but a greater temperature range needs to be covered to confirm this. For the IL with ester functionalised cation, $[\text{N}_{112,20\text{CO}1}][\text{Tf}_2\text{N}]$, Δ does show a definite temperature dependence, increasing from 0.25 to 0.35 with increasing temperature over just 40 K. Similar behaviour has been reported for $[\text{FSA}]^-$ and $[\text{Tf}_2\text{N}]^-$ salts of $[\text{Pyr}_{13}]^+$ and $[\text{emim}]^+$ by Hayamizu et al.^{39,40,53}

It is tempting to suggest that the effects described above are due in some way to the different morphologies of the mesoscopic structure of ionic liquids. It is known from X-ray scattering studies, for example, that there is a significant difference in intermediate range order between ionic liquids with alkyl and ethoxy-substituted cations, with a first sharp diffraction peak at 3 to 4 nm^{-1} apparent for the alkyl-substituted salts (with 1-hexyl-3-methylimidazolium, ammonium and phosphonium cations), but not the ethoxy- or hydroxyl-substituted analogues.⁵⁴ It was concluded in this study that the polar ether group causes the disappearance of mesoscopic structural correlations between the non-polar alkyl chains of the non-functionalised analogues. Canongia Lopes and co-workers have described ionic liquids as having both high-charge density and non-polar regions. Thus ILs based on 1-alkyl-3-methylimidazolium cations with long alkyl side-chains can form “globules” of polar and non-polar regions with H-bonding of cation and anion in favourable cases.⁵⁵ Substituted quaternary ammonium and phosphonium ions instead tend to form filamentous networks as the charge is largely centralised on the N or P moiety. Though theory has yet to establish a direct link between mesoscopic liquid structure

and the transport properties of ionic liquids and molten salts, it does appear that once the viscosity (or, indeed, any other transport property) is set by the ion interactions, the other transport properties scale accordingly, despite any differences in liquid structure. Thus the transport properties are better understood as functions of the viscosity rather than the state variables of temperature and density, *per se*.

Conclusions:

Ion self-diffusion coefficients have been measured for ionic liquids based on the cations *N*-acetoxyethyl-*N,N*-dimethyl-*N*-ethylammonium ($[N_{112,20CO1}]^+$) and its non-functionalised analogue, *N,N*-dimethyl-*N*-ethyl-*N*-pentylammonium ($[N_{1125}]^+$), and *N,N*-dimethyl-*N*-ethyl-*N*-methoxyethoxyethylammonium ($[N_{112,202O1}]^+$), and its analogue, *N,N*-dimethyl-*N*-ethyl-*N*-heptylammonium ($[N_{1127}]^+$) and the bis(trifluoromethanesulfonyl)amide anion. The functionalised chain on the ammonium cations has the same length, in terms of the number of atoms, as the non-functionalised chain of the corresponding analogue. For $[N_{112,20CO1}][Tf_2N]$ and $[N_{1127}][Tf_2N]$, the cation and anion self-diffusion coefficients are equal, within experimental error, whereas for $[N_{1125}][Tf_2N]$, the cation diffuses more quickly, and for $[N_{112,202O1}][Tf_2N]$, it is the anion that diffuses more quickly than the ether-functionalised cation. But these differences are relatively small, just beyond experimental error.

At a given temperature, the diffusion coefficients have magnitudes in the order $[N_{112,202O1}][Tf_2N] > [N_{1125}][Tf_2N] > [N_{1127}][Tf_2N] \sim [N_{112,20CO1}][Tf_2N]$. This is similar to the order for the molar conductivity, $[N_{112,202O1}][Tf_2N] > [N_{1125}][Tf_2N] >$

$[N_{112,20CO1}][Tf_2N] > [N_{1127}][Tf_2N]$, but not that for the fluidity ($\phi=1/\eta$), where $[N_{112,202O1}][Tf_2N] > [N_{1125}][Tf_2N] > [N_{1127}][Tf_2N] > [N_{112,20CO1}][Tf_2N]$.

The data are used to calculate velocity cross-correlation coefficients (VCC or f_{ij}) and distinct diffusion coefficients (D_{ij}^d). Both the self-diffusion and distinct diffusion coefficients are analysed in terms of (fractional) Stokes-Einstein-Sutherland equations. Though the self-diffusion coefficients, as with the conductivity and viscosity, show marked differences in absolute terms between the functionalised and non-functionalised forms, being higher for the ethoxy-substituted IL and lower for the acetoxy-substituted IL, these are largely removed by scaling with the viscosity. Thus the transport properties are better understood as functions of the viscosity rather than the temperature and density, *per se*. The presence of the alkoxy-substituted side chains is known to change the local mesoscopic liquid structure, but it appears once this is done, the transport properties scale in a corresponding way. In the case of the acetoxy-substituted IL, this is also largely the case, but the the Nernst-Einstein deviation parameter, Δ , which depends on the difference between the anion-cation VCC and the mean of the cation-cation and anion-anion VCCs, is smaller than that of its analogue salt, and also temperature dependent.

Acknowledgement.

The authors are grateful to Dr Kikuko Hayamizu (AIST, Tsukuba, Japan) for generously providing numerical diffusion data for $[N_{122,201}][Tf_2N]$. KRH acknowledges support from the (Australian) Prime Minister's Education Assistance Program for Japan in response to the Great East Japan Earthquake on 11 March 2011

and the generous hospitality of AIST, Sendai, and Nihon University, Koriyama, Fukushima, for a visit to Japan in March 2012.

Table 1. Substances and water content.

Substance	CAS no	$M / \text{g}\cdot\text{mol}^{-1}$	$10^6 \text{ wt fraction H}_2\text{O}$
[N ₁₁₂₅][Tf ₂ N]	1418127-14-6	424.424	37
[N _{112,20CO1}][Tf ₂ N]	1418127-13-5	440.380	46
[N ₁₁₂₇][Tf ₂ N]	1350984-18-7	452.477	49
[N _{112,202O1}][Tf ₂ N]	743436-72-8	456.423	45
Properties at 25 °C ²³	$V / \text{cm}^3\cdot\text{mol}$	$\eta / \text{mPa}\cdot\text{s}$	$\lambda / \mu\text{S}\cdot\text{m}^2\cdot\text{mol}^{-1}$
[N ₁₁₂₅][Tf ₂ N]	316.41	127.6	44.04
[N _{112,20CO1}][Tf ₂ N]	301.93	207.5	31.84
[N ₁₁₂₇][Tf ₂ N]	350.49	167.7	28.40
[N _{112,202O1}][Tf ₂ N]	328.10	58.57	84.36

Table 2. Coefficients for the VFT equation, (1)

	[N ₁₁₂₅][Tf ₂ N]		[N _{112,0CO1}][Tf ₂ N]		[N _{112,202O1}][Tf ₂ N]		[N ₁₁₂₇][Tf ₂ N]	
	D_+^{\ddagger}	D_-	D_+	D_-	D_+	D_-	D_+	D_-
A	8.149 ± 0.23	8.774 ± 0.55	9.399 ± 0.76	10.75 ± 0.80	9.625 ± 0.24	9.193 ± 0.46	9.275 ± 0.70	10.15 ± 1.2
B/K	-532.0 ± 54	-708 ± 159	-902 ± 233	-1333 ± 295	-956.7 ± 76	-863 ± 151	-896 ± 225	-1185 ± 428
T_0/K	210.1 ± 5.9	192.8 ± 16	181.3 ± 20	149.5 ± 20	155.8 ± 6.3	162.3 ± 14	178.2 ± 20	155.8 ± 32
st. devn/%	3.2	3.9	3.7	3.4	3.1	3.5	3.2	3.8
$T \text{ range } / ^\circ\text{C}$	30-90	40-90	40-90	35-91	10-90	25-91	40-90	40-90

[‡] $D_i / 10^{12} \text{m}^2 \text{s}^{-1}$

Table 3. Coefficients for the Litovitz equation, (2)

	[N ₁₁₂₅][Tf ₂ N]		[N _{112,0CO1}][Tf ₂ N]		[N _{112,2O2O1}][Tf ₂ N]		[N ₁₁₂₇][Tf ₂ N]	
	<i>D</i> ₊	<i>D</i> ₋	<i>D</i> ₊	<i>D</i> ₋	<i>D</i> ₊	<i>D</i> ₋	<i>D</i> ₊	<i>D</i> ₋
<i>A'</i>	7.8145 ± 0.046	7.7016 ± 0.041	7.8072 ± 0.050	7.8980 ± 0.044	7.6082 ± 0.021	7.4400 ± 0.035	7.6338 ± 0.042	7.6746 ± 0.049
<i>- B'/10⁶K³</i>	148.41 ± 1.6	147.41 ± 1.5	160.99 ± 1.9	163.08 ± 1.6	124.78 ± 0.62	121.94 ± 1.2	153.45 ± 1.6	155.69 ± 1.9
st. devn/%	4.4	4.0	3.1	3.5	3.1	3.5	3.2	3.9
<i>T</i> range /°C	30-90	40-90	40-90	35-91	10-90	25-91	40-90	40-90

Table 4. Parameters for Stokes-Einstein-Sutherland fits (Figure 4) of the self-diffusion coefficients, D_i , and the fluidity ($\phi = 1/\eta$) to $\ln(D_i/T) = x + t \ln(\phi)$

the $[N_{1125}][Tf_2N]$ and $[N_{112,20CO1}][Tf_2N]$ pair			
D_+ §		D_-	
x	1.244 ± 0.035	x	1.153 ± 0.036
t	0.978 ± 0.010	t	0.963 ± 0.011
st. devn/%	4.8	st. devn/%	5.3
the $[N_{1127}][Tf_2N]$ and $[N_{112,202O1}][Tf_2N]$ pair			
x	1.159 ± 0.027	x	1.130 ± 0.034
t	0.976 ± 0.007	t	0.989 ± 0.010
st. devn/%	5.1	st. devn/%	5.4

§ Units: $D_i/10^{-12} \text{ m}^2\text{s}^{-1}$, $\phi/(\text{Pa}\cdot\text{s})^{-1}$, T/K .

Table 5. Parameters for Stokes-Einstein-Sutherland fits (Figure 5) of the distinct diffusion coefficients, D_{ij}^d , and the fluidity ($\phi = 1/\eta$) to $\ln(D_{ij}^d/T) = x + t \ln(\phi)$

D_{++}^d **,††		D_{--}^d		D_{+-}^d	
[N ₁₁₂₅][Tf ₂ N]					
<i>x</i>	-5.672	<i>x</i>	-5.080	<i>x</i>	-5.976
<i>t</i>	1.040	<i>t</i>	0.986	<i>t</i>	0.939
[N _{112,0C01}][Tf ₂ N]					
<i>x</i>	-5.994	<i>x</i>	-5.100	<i>x</i>	-5.817
<i>t</i>	1.060	<i>t</i>	1.003	<i>t</i>	0.939
[N ₁₁₂₇][Tf ₂ N]					
<i>x</i>	-5.549	<i>x</i>	-5.180	<i>x</i>	-6.128
<i>t</i>	0.991	<i>t</i>	0.993	<i>t</i>	0.951
[N _{112,20201}][Tf ₂ N]					
<i>x</i>	-5.574	<i>x</i>	-5.131	<i>x</i>	-6.010
<i>t</i>	1.008	<i>t</i>	0.968	<i>t</i>	0.944

** Units: $D_{ij}^d / 10^{-12} \text{ m}^2 \text{ s}^{-1}$, $\phi / (\text{Pa} \cdot \text{s})^{-1}$, T/K .

†† The fitted parameters are calculated for smoothed values of the transport properties. The error in the slopes is estimated from experimental uncertainties at ± 0.04 for the like ion D_{ij}^d and ± 0.02 for the cation-anion D_{ij}^d .

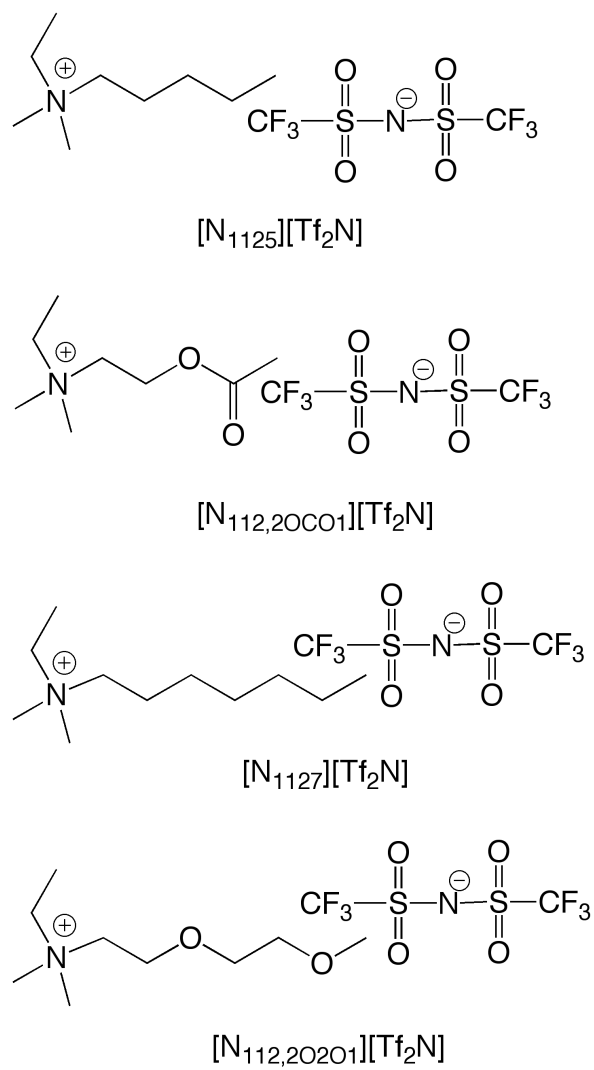


Fig. 1 Ionic liquid structures.

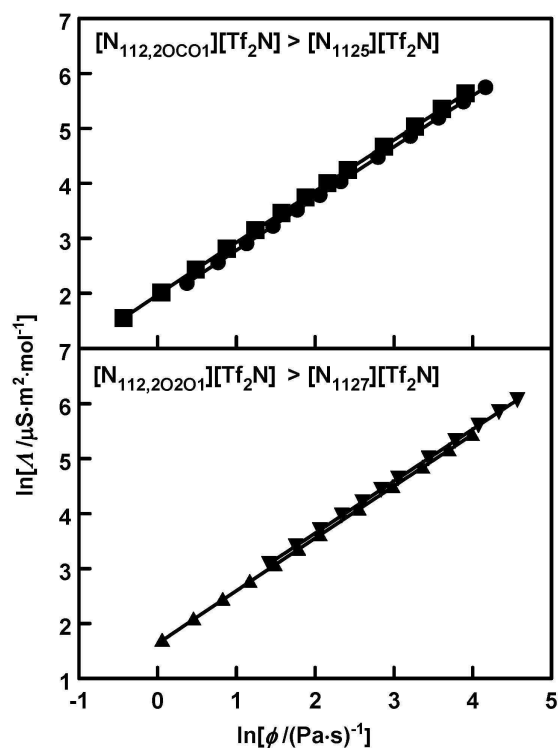


Fig. 2 Walden plot of molar conductivities (Λ) against fluidities ($\phi = 1/\eta$) for the pairs $[\text{N}_{1125}][\text{Tf}_2\text{N}]$ (\bullet), $t = 0.939$ and $[\text{N}_{112,20\text{CO}1}][\text{Tf}_2\text{N}]$ (\blacksquare), $t = 0.938$, (upper panel) and $[\text{N}_{1127}][\text{Tf}_2\text{N}]$ (\blacktriangle), $t = 0.951$, and $[\text{N}_{112,202\text{O}1}][\text{Tf}_2\text{N}]$ (\blacktriangledown), $t = 0.944$ (lower panel). The lines for $[\text{N}_{1125}][\text{Tf}_2\text{N}]$ (upper panel) and $[\text{N}_{112,202\text{O}1}][\text{Tf}_2\text{N}]$ (lower panel) are almost superposable on one another. Slopes, t , from ref. 23; standard deviation ± 0.002 .

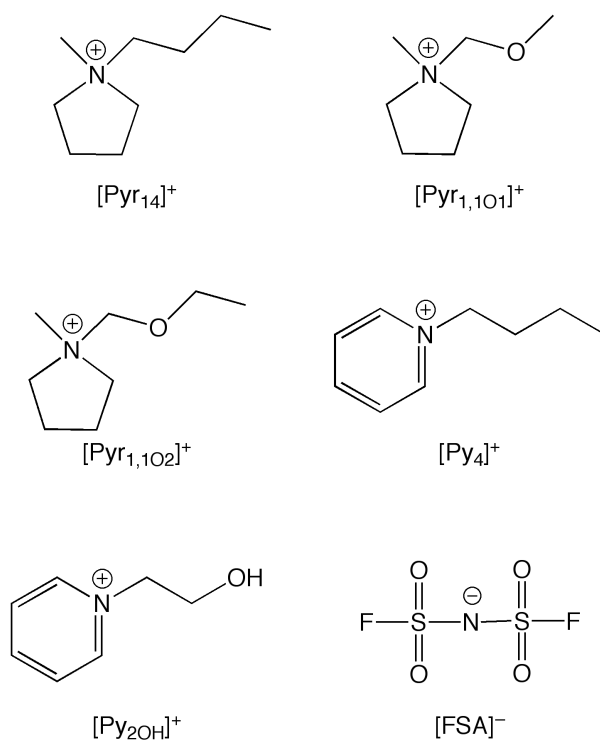


Fig. 3 Structures of pyroliidinium (Pyr) and pyridinium cations (Py) and the FSA anion

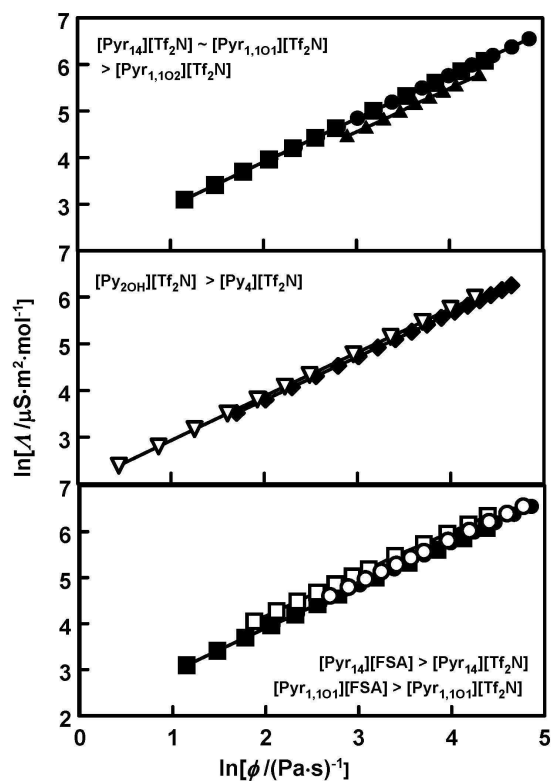


Fig. 4 Walden plot of molar conductivities (Λ) against fluidities ($\phi = 1/\eta$) for pyrrolidinium (Pyr) and pyridinium (Py) ionic liquids. $[\text{Pyr}_{14}][\text{Tf}_2\text{N}]$ (■), $t = 0.924$; $[\text{Pyr}_{1,101}][\text{Tf}_2\text{N}]$ (●), $t = 0.928$; $[\text{Pyr}_{1,102}][\text{Tf}_2\text{N}]$ (▲), $t = 0.931$; $[\text{Py}_{2\text{OH}}][\text{Tf}_2\text{N}]$ (▽), $t = 0.941$; $[\text{Py}_4][\text{Tf}_2\text{N}]$ (◆), $t = 0.927$; $[\text{Pyr}_{14}][\text{FSA}]$ (□), $t = 0.914$; and $[\text{Pyr}_{1,101}][\text{FSA}]$ (○), $t = 0.937$.

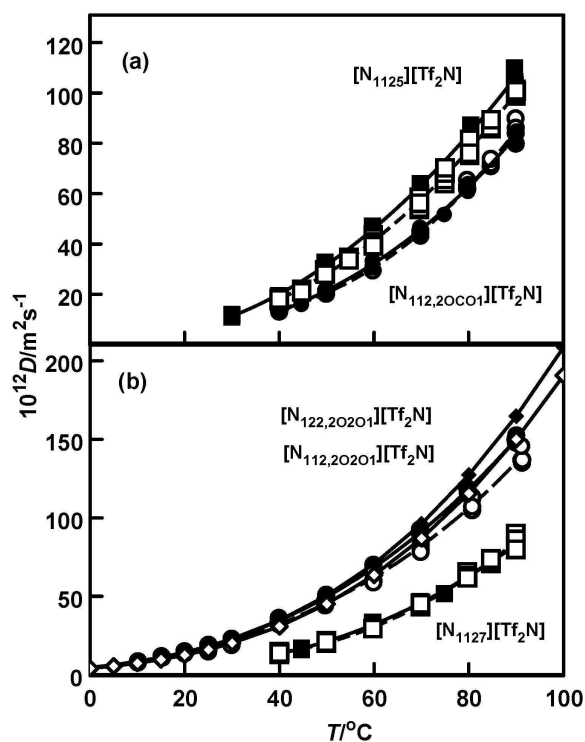


Fig. 5 Ion self-diffusion coefficients as a function of temperature: upper panel, (a), $[N_{1125}][Tf_2N]$ (squares) and $[N_{112,20CO1}][Tf_2N]$ (circles); lower panel, (b), $[N_{1127}][Tf_2N]$ (squares), $[N_{112,202O1}][Tf_2N]$ (circles), $[N_{122,202O1}][Tf_2N]$ (diamonds).⁴³ Symbols: solid, cation; open, anion. The $[N_{122,201}][Tf_2N]$ data were fitted to the VFT relation, Eq. (1): $D_+ / 10^{-12} \text{ m}^2\text{s}^{-1} = \exp(10.58 - 1279/(T/K - 131.2))$, stand. devn. = 5 %; $D_- / 10^{-12} \text{ m}^2\text{s}^{-1} = \exp(11.07 - 1446/(T/K - 123.6))$, stand. devn. = 6 %.

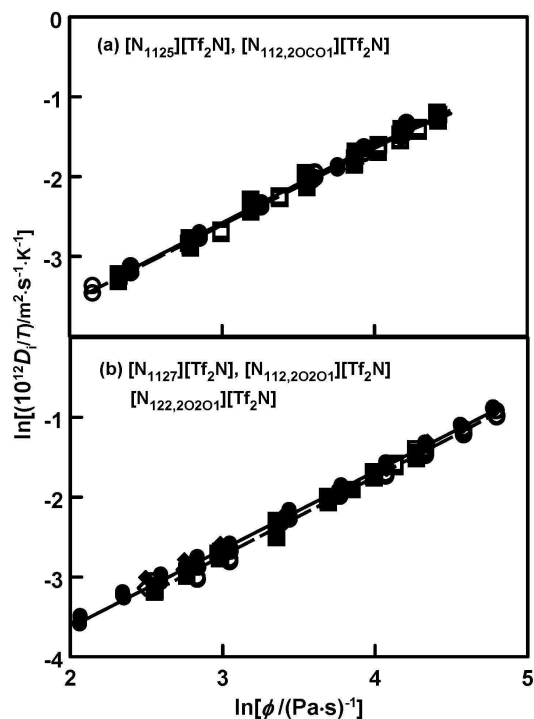


Fig. 6 Upper panel, (a): the effect of ester functionalisation: comparison at the same viscosity. Stokes-Einstein-Sutherland plot of ion self-diffusion coefficients as a function of fluidity ($\phi = 1/\eta$) for $[\text{N}_{1125}][\text{Tf}_2\text{N}]$ (squares) and $[\text{N}_{112,20\text{CO}1}][\text{Tf}_2\text{N}]$ (circles). Lower panel, (b): the effect of ether functionalisation: comparison at the same viscosity. Stokes-Einstein-Sutherland plot of ion self-diffusion coefficients as a function of fluidity ($\phi = 1/\eta$) for $[\text{N}_{1127}][\text{Tf}_2\text{N}]$ (squares), $[\text{N}_{112,202\text{O}1}][\text{Tf}_2\text{N}]$ (circles), and $[\text{N}_{122,201}][\text{Tf}_2\text{N}]$ (diamonds) (calculated from data in ref. 20 and 43). Symbols: solid, cation; open, anion. Parameters for the fits are given in Table 5.

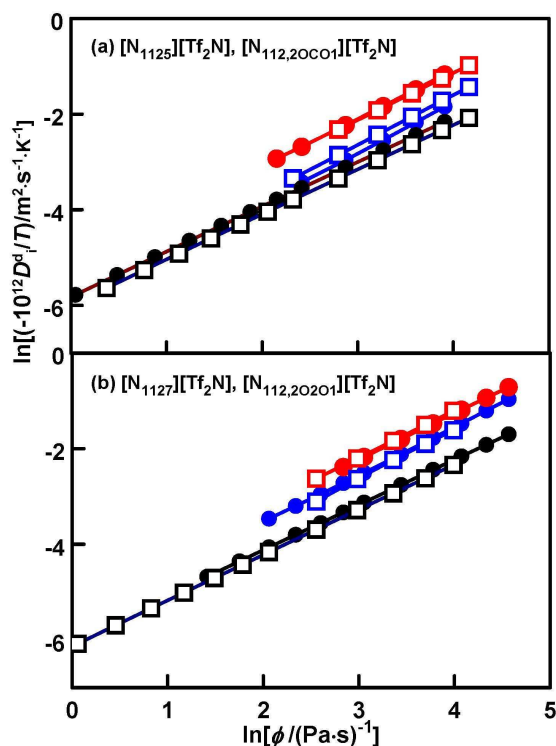


Fig. 7 Upper panel, (a): the effect of ester functionalisation: comparison at the same viscosity. Stokes-Einstein-Sutherland plot of ion liquid distinct diffusion coefficients as a function of fluidity ($\phi = 1/\eta$) for $[\text{N}_{1125}][\text{Tf}_2\text{N}]$ (squares) and $[\text{N}_{112,20\text{CO}1}][\text{Tf}_2\text{N}]$ (circles). Lower panel, (b): the effect of ether functionalisation: comparison at the same viscosity. Stokes-Einstein-Sutherland plot of ion liquid distinct diffusion coefficients as a function of fluidity ($\phi = 1/\eta$) for $[\text{N}_{1127}][\text{Tf}_2\text{N}]$ (squares) and $[\text{N}_{112,20\text{O}1}][\text{Tf}_2\text{N}]$ (circles). Symbols: black, cation-anion velocity cross-correlation; blue, cation-cation velocity cross-correlation; red, anion-anion velocity cross-correlation. Parameters for the fits are given in Table 5.

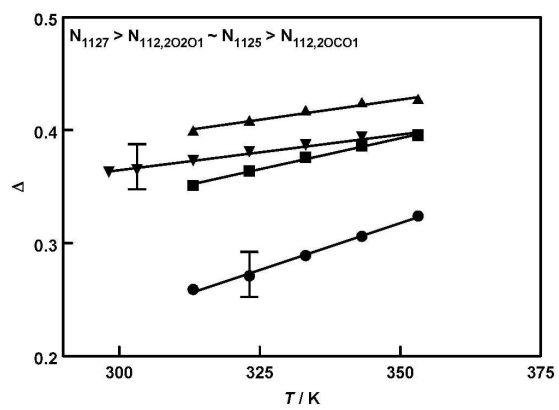


Fig. 8 Nernst-Einstein deviation parameter, Δ : symbols as in Figure 2.

-
- ¹ J. M. P. França, C. A. Nieto de Castro, M. Matos Lopes and V. M. B. Nunes, *J. Chem. Eng. Data*, 2009, **54**, 2569.
- ² S. Tang, G. A. Baker and H. Zhao, *Chem. Soc. Rev.*, 2012, **41**, 4030.
- ³ A.-L. Rollet and C. Bessada, *Annu. Rep. NMR Spectrosc.*, 2013, **78**, 149.
- ⁴ H. Tokuda, K. Hayamizu, K. Ishii, M. Abu Bin Hasan Susan and M. Watanabe, *J. Phys. Chem. B*, 2005, **109**, 6103.
- ⁵ Y. Jin, S. Fang, M. Chai, L. Yang and S. Hirano, *Ind. Eng. Chem. Res.*, 2012, **51**, 11011.
- ⁶ A. Martinelli, A. Maréchal, Å. Östlund and J. Cambedouzou, *Phys. Chem. Chem. Phys.*, 2013, **15**, 5510.
- ⁷ H. Shirota, H. Fukuzawa, T. Fujisawa and J. F. Wishart, *J. Phys. Chem. B*, 2010, **114**, 9400.
- ⁸ M. J. Monteiro, F. F. Camilo, M. C. C. Ribeiro and R. M. Torresi, *J. Phys. Chem. B*, 2010, **114**, 12488.
- ⁹ Z. J. Chen, T. Xue, and J.-M Lee, *RSC Advances*, 2012, **2**, 10564.
- ¹⁰ J. Reiter, S. Jeremias, E. Paillard, M. Winter and S. Passerini, *Phys. Chem. Chem. Phys.*, 2013, **15**, 2565.
- ¹¹ T. E. Thorpe and J. W. Rodger, *Proc. R. Soc. London*, 1894, **55**, 148.
- ¹² A. Bondi, *Ann. N. Y. Acad. Sci.*, 1951, **53**, 870.
- ¹³ L. C. Branco, L. N. Rosa, J. J. M. Ramos and C. A. M. Afonso, *Chem. Eur. J.*, 2002, **8**, 3671.
- ¹⁴ W. Xu, E. I. Cooper and C. A. Angell, *J. Phys. Chem. B*, 2003, **107**, 6170.
- ¹⁵ H. Niedermeyer, M. Azri Ab Rani, P. D. Lickiss, J. P. Hallett, T. Welton, A. J. P. White and P. A. Hunt, *Phys. Chem. Chem. Phys.*, 2010, **12**, 2018.
- ¹⁶ L. J. A. Siquera and M. C. C. Ribeiro, *J. Phys. Chem. B*, 2009, **113**, 1074.
- ¹⁷ M. H. Kowsari, S. Alavi, B. Najafi, K. Gholizadeh, E. Dehghanpisheh and F. Ranjbar, *Phys. Chem. Chem. Phys.*, 2011, **13**, 8826.
- ¹⁸ K. R. Harris, *J. Phys. Chem. B*, 2010, **114**, 9572.
- ¹⁹ T. Umecky, Y. Saito, S. Tsuzuki and H. Matsumoto, *Electrochem. Soc. Trans.*, 2009, **16**, 39.
- ²⁰ Y. Yoshida and G. Saito, *Phys. Chem. Chem. Phys.*, 2011, **13**, 20302.

-
- ²¹ N. Terasawa, S. Tsuzuki, T. Umecky, Y. Saito and H. Matsumoto, *Chem. Commun.*, 2010, **46**, 1730.
- ²² U. A. Rana, R. Vijayaraghavan, M. Walther, J.-Z. Sun, A. A. J. Torriero, M. Forsyth and D. R. MacFarlane, *Chem. Commun.*, 2011, **47**, 11612.
- ²³ J. Luo, O. Conrad and I. F. J. Vankelecom, *J. Materials Chem.*, 2012, **22**, 20574.
- ²⁴ K. Tsunashima, M. Fukushima and M. Matsumiya, *Electrochemistry (Tokyo, Jpn)*, 2012, **80**, 904.
- ²⁵ T. Makino, M. Kanakubo, T. Umecky and A. Suzuki, *J. Chem. Eng. Data*, 2013, **58**, 370.
- ²⁶ T. Makino, M. Kanakubo, T. Umecky, A. Suzuki, T. Nishida and J. Takano, *J. Chem. Eng. Data*, 2012, **57**, 751.
- ²⁷ M. Kanakubo, K. R. Harris, N. Tsuchihashi, K. Ibuki and M. Ueno, *J. Phys. Chem. B*, 2007, **111**, 2062.
- ²⁸ M. Kanakubo, K. R. Harris, N. Tsuchihashi, K. Ibuki and M. Ueno, *J. Phys. Chem. B*, 2008, **112**, 9830.
- ²⁹ H. Schönert, *J. Phys. Chem.*, 1984, **88**, 3359.
- ³⁰ H. L. Friedman and R. Mills, *J. Sol. Chem.*, 1981, **10**, 395.
- ³¹ K. R. Harris, L. A. Woolf, M. Kanakubo and T. Rütger, *J. Chem. Eng. Data*, 2011, **56**, 4672.
- ³² K. R. Harris and M. Kanakubo, *Faraday Disc.*, 2012, **154**, 425.
- ³³ T. Rütger, K. R. Harris, M. D. Horne, M. Kanakubo, T. Rodopoulos, J.-P. Veder and L. A. Woolf, *Chem. Eur. J.*, in press, DOI: 10.1002/chem.201302258.
- ³⁴ F. S. Oliveira, M. G. Freire, P. J. Carvalho, J. A. P. Coutinho, J. N. Canongia Lopes, L. P. N. Rebelo and I. M. Marrucho, *J. Chem. Eng. Data*, 2010, **55**, 4514.
- ³⁵ H. Tokuda, S. Tsuzuki, M. Abu Bin Hasan Susan, K. Hayamizu and M. Watanabe, *J. Phys. Chem. B*, 2006, **110**, 19593.
- ³⁶ T. Makino, M. Kanakubo, T. Umecky and A. Suzuki, *Fluid Phase Equil.*, 2013, **357**, 64.
- ³⁷ F. M. Gaciño, T. Regueira, L. Lugo, M. J. P. Comuñas and J. Fernández, *J. Chem. Eng. Data*, 2011, **56**, 4984.
- ³⁸ S. Bulut, P. Eiden, W. Beichel, J. M. Slattery, T. F. Beyersdorff, T. J. S. Schubert and I. Krossing, *ChemPhysChem*, 2011, **12**, 2296.

- ³⁹ K. Hayamizu, S. Tsuzuki, S. Seki and Y. Umebayashi, *J. Chem. Phys.*, 2011, **134**, 084505.
- ⁴⁰ K. Hayamizu, S. Tsuzuki, S. Seki, K. Fujii, M. Suenaga and Y. Umebayashi, *J. Chem. Phys.*, 2010, **133**, 194505.
- ⁴¹ K. Hayamizu, S. Tsuzuki and S. Seki, *J. Phys. Chem. A*, 2008, **112**, 12027.
- ⁴² K. Hayamizu, On Accurate Measurements of Diffusion Coefficients by PGSE NMR Methods - Room-Temperature Ionic Liquids.
http://www.ribm.co.jp/service/nmr_document/pgse-nmr_eng.pdf. Accessed on 18 Jan 2014.
- ⁴³ K. Hayamizu, S. Tsuzuki, S. Seki, Y. Ohno, H. Miyashiro and Y. Kobayashi, *J. Phys. Chem. B*, **2008**, *112*, 1189.
- ⁴⁴ J. M. Slattery, C. Daguinet, P. J. Dyson, T. J. S. Schubert and I. Krossing, *Angew. Chem. Int. Ed.*, 2007, **46**, 5384.
- ⁴⁵ J. A. P. Coutinho, P. J. Carvalho and N. M. C. Oliveira, *RSC Advances*, 2012, **2**, 7322.
- ⁴⁶ C. M. Roland, J. L. Feldman and R. Casalini, *J. Non-Cryst. Solids*, 2006, *352*, 4895.
- ⁴⁷ Ingebrigtsen, T. S.; Schröder, T. B.; and Dyre, J. C. *Phys. Rev. X*, 2012, **2**, 011011.
- ⁴⁸ E. R. López, A. S. Pensado, M. J. P. Comuñas, A. A. H. Pádua, J. Fernández and K. R. Harris, *J. Chem. Phys.*, 2011, **134**, 144507.
- ⁴⁹ H. K. Kashyap, H. V. R. Annapureddy, F. O. Raineri and C. J. Margulis, *J. Phys. Chem. B*, 2011, **115**, 13212.
- ⁵⁰ L. A. Woolf and K. R. Harris, *J. Chem. Soc., Faraday Trans. 1*, 1978, **74**, 933.
- ⁵¹ J. O'M. Bockris, E. H. Crook, H. Bloom and N. E. Richards, *Proc. Roy. Soc. A*, 1960, **225**, 558.
- ⁵² J. O'M. Bockris and G. W. Hooper, *Discuss. Faraday Soc.*, 1961, **32**, 218.
- ⁵³ In the case of the [Pyr]⁺ salts, the Stokes-Einstein-Sutherland plots are unexpectedly non-linear, except for D_{-}^d for [Pyr₁₃][FSA] and D_{+}^d for both [Pyr₁₃][FSA] and [Pyr₁₃][Tf₂N].
- ⁵⁴ A. Triolo, O. Russina, R. Caminiti, H. Shirota, H. Y. Lee, C. S. Santos, N. S. Murthy, and E. W. Castner, Jr, *Chem. Comm.*, 2012, **48**, 4959.
- ⁵⁵ K. Shimizu, C. E. S. Bernardes, A. Triolo and J. N. C. Lopes, *Phys. Chem. Chem. Phys.*, 2013, **15**, 16256.